VIP Transmembrane Molecular Recognition Very Important Paper

International Edition: DOI: 10.1002/anie.201502677
German Edition: DOI: 10.1002/ange.201502677

Recruitment and Immobilization of a Fluorinated Biomarker Across an Interfacial Phospholipid Film using a Fluorocarbon Gas**

*Guang Yang, Miriam O'Duill, Véronique Gouverneur, and Marie Pierre Krafft**

Abstract: *Perfluorohexane gas when introduced in the air atmosphere above a film of phospholipid self-supported on an aqueous solution of C_2F_5-labeled compounds causes the recruitment and immobilization of the latter in the interfacial film. When the phospholipid forms a liquid-condensed Gibbs monolayer, which is the case for dipalmitoylphosphatidylcholine (DPPC), the C_2F_5-labeled molecule remains trapped in the monolayer after removal of F-hexane. Investigations involve bubble profile analysis tensiometry (Gibbs films), Langmuir monolayers and microbubble experiments. The new phenomenon was utilized to incorporate a hypoxia biomarker, a C_2F_5-labeled nitrosoimidazole (EF5), in microbubble shells. This finding opens perspectives in the delivery of fluorinated therapeutic molecules and biomarkers.*

Phospholipid films and membranes are ubiquitous at cellular interfaces in living organisms. Monolayers of phospholipids, self-supported at the air/water interface, are effective models for investigating the recognition, recruitment, and organization of biological and therapeutic water-soluble molecules at interfaces.[1] So far, the strategies implemented to prompt the selective adsorption of biologically active species at a phospholipid/air interface have essentially used directional driving forces such as hydrogen bonding and/or electrostatic forces. It is striking that hydrophobic interactions, which are central to many essential biological processes, including those involving molecular recognition, have never, to our knowledge, been used to promote the adsorption of water-soluble molecules on phospholipid films.

The most powerful hydrophobic interactions known are those developed by perfluoroalkylated (*F*-alkyl) compounds.[2] Although the mutual interactions between fluorinated chains are notoriously weak, effective attractive interactions can operate in water and organic solvents. Examples of implementation of such interactions include the temperature-driven segregation and partition of *F*-alkyl chains, which are the basis for "fluorous" technologies used in many synthesis and separation procedures.[3] All known examples of such interactions are limited to liquid/liquid and solid/liquid interfaces.[4,5] By contrast, the potential of fluorocarbon gases to develop attractive interactions towards fluorinated molecules solubilized in a liquid phase across a molecular film at a gas/water interface has not been investigated. Yet, this situation is of interest when delivering fluorinated drugs or biotracers. Fluorinated pharmaceuticals (with a fluorine atom, a CF_3 or C_2F_5 group) reach 20% of the total marketed drugs.[6] The possibility of immobilizing such drugs in phospholipid monolayers would enable their incorporation in the shell of medical microbubbles, which are often shelled with phospholipids and osmotically stabilized by a fluorocarbon gas. Microbubbles are versatile colloidal carriers potentially useful for multi-modal diagnosis, targeted therapy and theranostics.[7]

Here, we first report that the adsorption of the water-soluble alcohol $C_2F_5(CH_2)_4OH$ (F5OH) onto an interface covered by a phospholipid monolayer can be profoundly modified by introducing the poorly water-soluble perfluorohexane (*F*-hexane) in the gas phase. *F*-hexane causes the adsorption of F5OH into the phospholipid monolayer, which does not occur in its absence. This phenomenon is assigned to attractive interactions between fluorinated chains operating across the phospholipid film. It represents a new type of transmembrane molecular "recognition" in which a fluorocarbon gas provokes the immobilization in the interfacial film of fluorinated molecules initially dissolved in the aqueous phase.

Next, in order to assess the generality of the observed phenomenon and its applicability to drug and biotracer delivery, we studied the effect of *F*-hexane on the adsorption of a biologically relevant fluorinated compound. We selected a fluorinated nitrosoimidazole (EF5), a hypoxia marker that, when radiolabeled with ^{18}F, is in clinical studies for the early diagnosis of tumours using positron emission tomography (PET).[8]

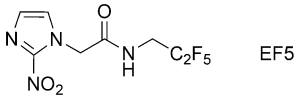

EF5

EF5 (synthesized according to reference [9]) is a good candidate for our purpose as its insertion in the shell of microbubbles would provide a dual-mode PET/ultrasound imaging agent. PET has been used to investigate the biodistribution of microbubbles radiolabeled with ^{18}F.[10] We show that *F*-hexane efficiently promotes the immobilization of EF5 in a phospholipid monolayer, whilst no adsorption occurs in its absence. We successfully apply this recruitment

[*] G. Yang, Dr. M. P. Krafft
Institut Charles Sadron (CNRS), University of Strasbourg
23 rue du Loess, 67034 Strasbourg (France)
E-mail: krafft@unistra.fr
M. O'Duill, Prof. V. Gouverneur
Chemistry Research Laboratory, University of Oxford
12 Mansfield Road, Oxford OX1 3TA (UK)

[**] We thank the French National Research Agency (ANR-14-CE35-0028-01) for funding, and Teclis Instruments (Longessaigne, France) for discussion and technical help.

Supporting information for this article is available on the WWW under http://dx.doi.org/10.1002/anie.201502677.

 © 2015 Wiley-VCH Verlag GmbH & Co. KGaA, Weinheim

principle to immobilizing EF5 in the phospholipid shells of microbubbles.

Experiments were run on spontaneously adsorbed (Gibbs) and spread (Langmuir) interfacial phospholipid films, with and without *F*-hexane present in the gas phase. Two phospholipids were investigated: dioctanoylphosphatidylcholine (diC_8PC), a short-chain micelle-forming phospholipid, and dipalmitoylphosphatidylcholine (DPPC), a long-chain one that forms vesicles and is a major component of cell membranes.

Bubble profile analysis tensiometry[11] was used to determine the sequential kinetic adsorption profiles of F5OH and EF5 on a monolayer of phospholipid pre-adsorbed on a millimetric air bubble that was saturated—or not—with *F*-hexane (Scheme 1).

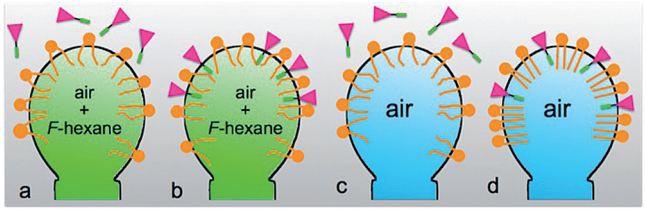

Scheme 1. Adsorption scenarios for C_2F_5-labeled compounds at the surface of a phospholipid-covered rising air bubble. a) F5OH or EF5 (red triangles with green tails) is injected in the aqueous phase at a chosen time-point, and allowed to adsorb in the diC_8PC, or DPPC, monolayer, the air bubble being saturated with *F*-hexane. b) The C_2F_5-labeled compound is immobilized in the phospholipid monolayer. c) Replacement of *F*-hexane by air leads to ejection of the C_2F_5-labeled compound when the monolayer is in the liquid-expanded phase. d) On the other hand, it remains trapped when the phospholipid is in the liquid-condensed phase. Not on scale.

We first examined the adsorption behaviour of each compound separately. When present in the bubble's gas phase, *F*-hexane adsorbs rapidly on the surface of the Hepes buffer, as shown by an immediate reduction of the interfacial tension γ by $3 \pm 0.5\ mN\,m^{-1}$ (Supporting Information (SI), Figure S1). F5OH solubilized in the aqueous phase adsorbs weakly at the interface, reducing γ slowly from 70 to $57\ mN\,m^{-1}$ ($1 \times 10^{-4}\ mol\,L^{-1}$, Figure 1 inset). When *F*-hexane is present, the adsorption of F5OH is significantly faster (Figure 1 inset; characteristic time $t_1 = 450 \pm 50$ s versus 700 ± 50 s when *F*-hexane is absent), but the interfacial tension at equilibrium (γ_{eq}) is not changed. The characteristic time t_1 was determined by fitting the experimental curve with an exponential decay function. The acceleration of adsorption induced by *F*-hexane was seen over a large range of concentrations (SI, Figure S2). The adsorption of diC_8PC, solubilized in the aqueous phase, is also significantly accelerated by *F*-hexane (Figure 1, curves a_0 and a_F; $t_1 = 400$ s versus 60 s) and γ_{eq} is decreased slightly (see reference [12]). Acceleration of the kinetics and lowering of γ are also seen for a range of concentrations (SI, Figure S3).

Next, we investigated the effect of the fluorocarbon gas on the sequential adsorption of diC_8PC and F5OH at the interface using the following scenario. The phospholipid is allowed to adsorb first. The diC_8PC monolayer is in a liquid-expanded phase (LE) throughout the course of its adsorption, as reflected by a very low viscoelastic modulus E ($10 \pm 2\ mN\,m^{-1}$). F5OH is injected in the aqueous phase 500 s later. In the absence of *F*-hexane, the injection of F5OH has no notable effect on the adsorption profile of the phospholipid (Figure 1, curves a_0 and b_0). F5OH does not adsorb, likely because diC_8PC has already colonized the interface, preventing the alcohol from acceding. Surprisingly, the outcome of the sequential adsorption is profoundly changed when *F*-hexane is present in the bubble's inner gas phase (Figure 1, curve b_F). About 5 min after the addition of F5OH, γ is seen to decrease strongly (by $15 \pm 1\ mN\,m^{-1}$) and stabilizes at $40\ mN\,m^{-1}$, a value far below that reached by diC_8PC and F5OH taken separately. This indicates that F5OH penetrates in the phospholipid monolayer ($t_1 = 900 \pm 80$ s) and that a synergy takes place between the two compounds.

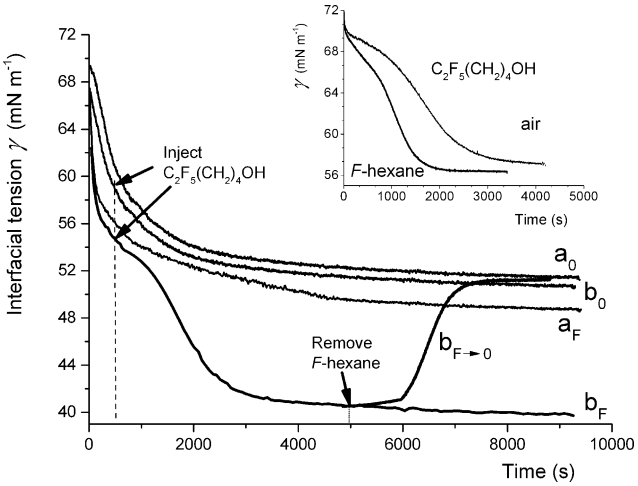

Figure 1. Kinetics of a) adsorption of diC_8PC and b) sequential adsorption of diC_8PC followed by F5OH (injected after 500 s, arrows). The experiments were achieved in the presence ($_F$), or absence ($_0$), of *F*-hexane. The subscript ($_{F\to0}$) refers to an experiment in which *F*-hexane is displaced by air, while keeping constant the bubble volume. Concentrations: $1 \times 10^{-4}\ mol\,L^{-1}$ for F5OH; $2.5 \times 10^{-6}\ mol\,L^{-1}$ for diC_8PC; 25 °C. Inset: adsorption profile of F5OH at the air/water and *F*-hexane-saturated air/water interface.

In order to better define the phenomenon, we have replaced *F*-hexane by air in the bubble's gas phase after 5000 s (Figure 1, curve $b_{F\to0}$). Our tensiometer is equipped with a module consisting of two syringes connected to a coaxial double capillary system, which allows the exchange of the bubble gas, while keeping its volume constant (see SI). After ca. 5 min, γ increases rapidly and plateaus at $52\ mN\,m^{-1}$, a typical value for diC_8PC alone. This means that, when *F*-hexane is removed, F5OH is totally ejected from the phospholipid monolayer. Furthermore, experiments run with octanol instead of F5OH did not reveal any effect on the diC_8PC monolayer. Likewise, *n*-hexane vapors did not promote adsorption of F5OH in the diC_8PC monolayer (SI, Figure S4). These results strongly suggest that attractive interactions between *F*-hexane and the C_2F_5 group of F5OH are responsible for the immobilization of the latter at the interface.

© 2015 Wiley-VCH Verlag GmbH & Co. KGaA, Weinheim

The behavior of the larger *F*-nitrosoimidazole EF5 tracer, in which the relative weight of the fluorocarbon moiety is smaller, was then examined. EF5 alone adsorbs slowly and weakly at the interface (Figure 2 inset; see SI for other concentrations, Figure S5). *F*-hexane strongly accelerated EF5 adsorption (Figure 2 inset; $t_1 = 750 \pm 50$ s versus 300 ± 50 s, see SI for example of fit, Figure S6). No significant influence was seen on γ_{eq}. In sequential adsorption experiments, the injection of EF5 in the aqueous phase, 500 s after the formation of a diC_8PC-covered *F*-hexane-saturated bubble, caused γ to decrease by 10 ± 1 mN m^{-1} within 10 min (Figure 2, curve b_F). Paralleling the behavior observed with F5OH, EF5 adsorbs in the diC_8PC monolayer, forming a mixed monolayer ($t_1 = 900 \pm 80$ s). As with F5OH, *n*-hexane has no effect on the adsorption of EF5 on the monolayer. Replacement of *F*-hexane by air leads to ejection of EF5 from the monolayer (Figure 2, curve $b_{F\to0}$). This is likely due to the fact that the interactions in the dilute monolayer of diC_8PC, in which exchanges with the water bulk phase occurs, are too weak to maintain EF5.

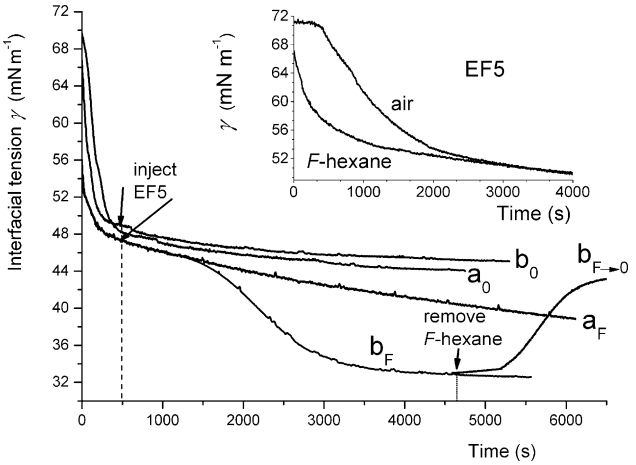

Figure 2. Kinetics of a) adsorption of diC_8PC and b) sequential adsorption of diC_8PC followed by EF5 (injected after 500 s, arrows). See Figure 1 for meaning of subscripts. Concentrations: 5×10^{-6} mol L^{-1} for diC_8PC; 1×10^{-3} mol L^{-1} for EF5; 25 °C. Inset: adsorption profile of EF5 alone at the air/water and *F*-hexane-saturated air/water interface.

Next we questioned whether this phenomenon is observed for biologically "more realistic" phospholipids such as those that form vesicles at low concentrations and display phase transitions. Therefore, we studied the effect of EF5 on a monolayer of DPPC, a phospholipid ubiquitous in cell membranes and broadly used in medical microbubbles. DPPC monolayers exhibit a transition from a dilute liquid-expanded (LE) phase to a liquid-condensed (LC) phase upon compression. We can thus investigate the recruitment and immobilization effect of *F*-hexane towards EF5 across a phospholipid monolayer in both dilute and condensed states. DPPC was provided in the form of narrowly dispersed small vesicles (60–80 nm). For this slow-adsorbing phospholipid, the bubble was submitted to sinusoidal oscillations (period T 10 s; surface area amplitude ΔA 15 %). Such an oscillatory regime was shown to strongly accelerate DPPC adsorption, thus enabling bubble profile analysis studies with vesicle-forming phospholipids.[13] The LE/LC transition is clearly seen (52 mN m^{-1}; 1 h) on the adsorption profile, both in the presence, or absence of *F*-hexane (Figure 3, curves a_0 and a_F). The introduction of *F*-hexane strongly accelerates the adsorption of DPPC (Figure 3, compare a_0 and a_F; $t_1 = 650 \pm 50$ s versus 200 ± 30 s). An aqueous solution of EF5 is injected into the aqueous phase at two time-points after the formation of the bubble in the DPPC vesicle-containing phase: 500 s (monolayer in the LE phase, $E = 50$ mN m^{-1}) and 7000 s (monolayer in the LC phase, $E = 200$ mN m^{-1}). When EF5 is injected after 500 s, the LE/LC transition is suppressed (curve b_F) and γ decreases immediately to a low value (25 mN m^{-1}), showing formation of the mixed EF5/DPPC monolayer. When EF5 is injected 7000 s after bubble formation (curve c_F), γ decreases very rapidly, after a time lag of ca. 1 h, and reaches the same low value of 25 mN m^{-1} ($t_1 = 900 \pm 80$ s). This proves that in the presence of *F*-hexane EF5 adsorbs, and forms a mixed monolayer with the phospholipid, whether the monolayer is in the LE or LC phase. The γ values of the mixed monolayers after equilibration are very similar and do not change for hours, indicating that they are at equilibrium. By contrast with the dilute diC_8PC monolayers, replacement of *F*-hexane by air has no effect: EF5 remains immobilized in the DPPC monolayer, whether initially in the LE or the LC phases (curves $b_{F\to0}$ and $c_{F\to0}$ versus a_F).

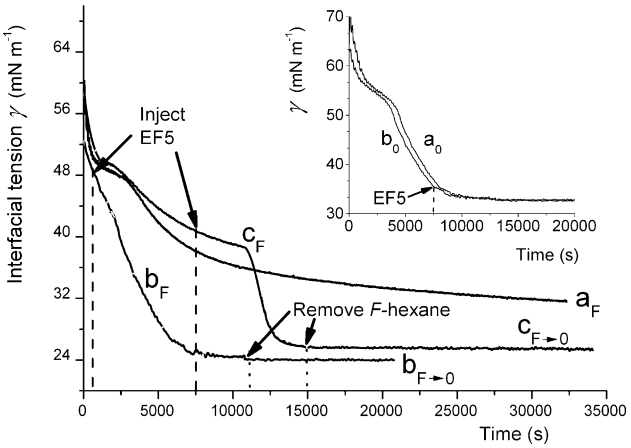

Figure 3. Kinetics of a) adsorption of DPPC and b,c) sequential adsorptions of DPPC followed by EF5 injected after 500 s (b), or 7000 s (c). See Figure 1 for meaning of subscripts. Concentrations: 1×10^{-3} mol L^{-1} for both DPPC and EF5; 37 °C. Inset: a) adsorption kinetics of DPPC and b) sequential adsorption of DPPC and EF5 (injected 7000 s after formation of the bubble). These experiments were run in the absence of *F*-hexane.

How strong are the interactions within the C_2F_5-labeled tracer/*F*-hexane/phospholipid mixed film? Langmuir monolayers allow assessing the stability of gas/water interfacial films upon compression by measuring their surface pressure at collapse (π_c). DPPC monolayers were spread on water in a Langmuir trough enclosed in a tight box, allowing saturation of the gas phase with *F*-hexane.[14] EF5 was injected in the subphase just prior to compression (Figure 4).

When *F*-hexane is present, the apparent molecular area A of DPPC alone is strongly shifted towards the large values,

 © 2015 Wiley-VCH Verlag GmbH & Co. KGaA, Weinheim

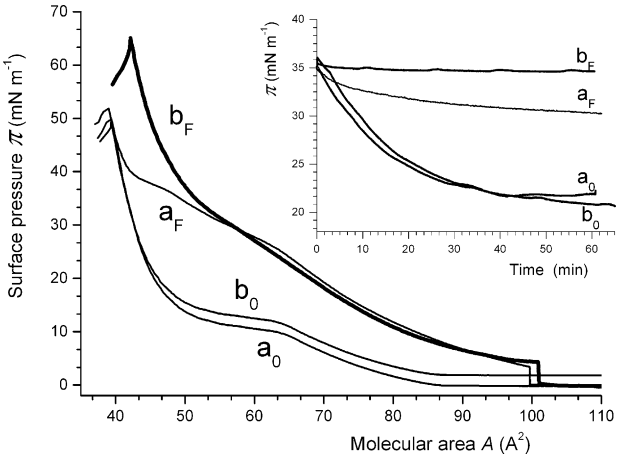

Figure 4. Surface pressure (π)/molecular area (A) isotherms of DPPC Langmuir monolayers compressed over a) an aqueous sub-phase or b) a sub-phase into which EF5 is injected before compression. See Figure 1 for meaning of subscripts. Inset: the monolayers are compressed up to 36 mN m^{-1}. The compression is stopped and the variation of π is monitored over time. EF5 concentration: 1×10^{-3} mol L^{-1}; 25 °C.

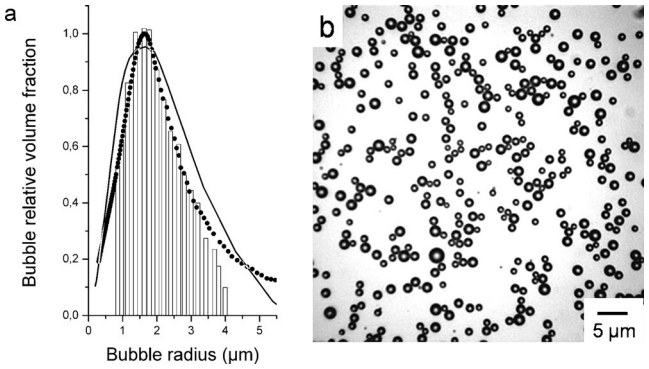

Figure 5. a) Size distributions of *F*-hexane-stabilized microbubbles with EF5 inserted in their diC$_8$PC shells after one week at 25 °C: optical microscopy (bar histogram), static light scattering (line), acoustical attenuation (circles). b) Optical micrograph of microbubbles after one week at 25 °C.

consistent with insertion of *F*-hexane in the monolayer (curves a_0 and a_F). However, further compression causes A to recover its initial value, indicating that *F*-hexane has been totally expelled from the film at high surface pressure π. In contrast, with EF5 in the sub-phase and *F*-hexane in the gas phase, A remains larger than for pure DPPC even at high π, showing that EF5 remains inserted in the monolayer (curve b_F). The decisive role of *F*-hexane in recruiting EF5 in the DPPC film is supported by the fact that, in the absence of *F*-hexane (curve b_0), there is no detectable difference in the isotherm. π_c was higher for the mixed DPPC/EF5 monolayer (65 versus 50 mN m^{-1}), indicating higher stability. Higher stability was also demonstrated by compressing the mixed monolayers at a given π, then monitoring π variation over time (Figure 4 inset). These results provide unambiguous evidence that strong attractive interactions exist between *F*-hexane and EF5 that enable EF5 immobilisation into the phospholipid monolayer even under severe compression (ca. 50 %).

A further important question is whether the attractive effect of *F*-hexane vis-à-vis of EF5, and its subsequent immobilization, could be operative in gas microbubbles. We therefore prepared microbubbles with a diC$_8$PC shell and stabilized (or not) with *F*-hexane, as reported before.[15] EF5 was introduced in the aqueous phase immediately after preparation (see SI). Without EF5, unstable bubbles are formed that disappear within minutes, whether *F*-hexane is present or not. The "over-compression" of the shell due to rapid dissolution of the soluble gases in water results in the redissolution of diC$_8$PC, as known for soluble surfactants.[16] When EF5 and *F*-hexane are both present, the microbubbles become stable enough to withstand centrifugation and resuspension in the aqueous solution. Monomodal populations of small and narrowly dispersed microbubbles (2.2 ± 0.4 μm in radius) were obtained that remain stable for over one week at 25 °C without significant change in size (Figure 5).

The co-presence of diC$_8$PC, EF5 and *F*-hexane in the bubbles' shell was confirmed by FTIR, which shows simultaneous characteristic vibrations (cm^{-1}) for diC$_8$PC (ester: 1728; *sym* and *asym* PO_2^-: 1246 and 1075; C–C–N$^+$: 966), EF5 (amide C=O: 1684; N–O: 1537, 1364; C–F: 1194, 1141, narrow), and *F*-hexane (C-F: 1201, 1148, broad). The ratio of the area of the N–O to C–F bands (5.4) is 2.3 times larger in the bubble shell than in EF5 (2.4), confirming the presence of *F*-hexane (SI, Figure S7).

In summary, when a phospholipid film is present at a *F*-hexane-saturated air/water interface, *F*-hexane penetrates in this film. C_2F_5-labeled compounds initially solubilized in the aqueous phase are attracted to the interface due to the hydrophobic effect. They are then immobilized in the film owing to attractive fluorocarbon–fluorocarbon interactions. When the monolayers are in a LE phase (diC$_8$PC), replacement of *F*-hexane by air leads to ejection of the C_2F_5-labeled compounds. By contrast, they remain trapped in LC monolayers (DPPC). A C_2F_5-labeled biomarker (EF5) is effectively immobilized in bubble shells when, and only when *F*-hexane is present. Since most medical microbubbles have a phospholipid shell and are stabilized by a fluorocarbon gas, our data support a novel and efficient means of immobilizing fluorinated drugs and biomarkers in microbubbles. The drug would not be covalently bound, allowing delivery by using a mechanical stimulus such as an ultrasound pulse.

Keywords: drug delivery · fluorocarbons · microbubbles · molecular recognition · phospholipid interfaces

How to cite: *Angew. Chem. Int. Ed.* **2015**, *54*, 8402–8406
Angew. Chem. **2015**, *127*, 8522–8526

[1] K. Ariga, T. Kunitake, *Acc. Chem. Res.* **1998**, *31*, 371–378.
[2] H. Ringsdorf, B. Schlarb, J. Venzmer, *Angew. Chem. Int. Ed. Engl.* **1988**, *27*, 113–158; *Angew. Chem.* **1988**, *100*, 117–162; B. E. Smart in *Organofluorine Chemistry: Principles and Commercial Applications* (Eds.: R. E. Banks, B. E. Smart, J. C. Tatlow), Plenum, New York, **1994**, chap. 3, pp. 57–88; M. P. Krafft, J. G. Riess, *Chem. Rev.* **2009**, *109*, 1714–1792.
[3] *Handbook of Fluorous Chemistry* (Eds.: J. A. Gladysz, D. P. Curran, I. Horváth), Wiley-VCH, Weinheim, **2004**.

 © 2015 Wiley-VCH Verlag GmbH & Co. KGaA, Weinheim

[4] Z. Luo, Q. Zhang, Y. Oderaotoshi, D. P. Curran, *Science* **2001**, *291*, 1766 – 1769; R. Bejot, L. Carroll, K. Bhakoo, J. Declerck, V. Gouverneur, *Bioorg. Med. Chem.* **2012**, *20*, 324 – 329.
[5] L. V. Dinh, J. Gladysz, *Angew. Chem. Int. Ed.* **2005**, *44*, 4095 – 4097; *Angew. Chem.* **2005**, *117*, 4164 – 4167.
[6] S. Purser, P. R. Moore, S. Swallow, V. Gouverneur, *Chem. Soc. Rev.* **2008**, *37*, 320 – 330.
[7] S. Sirsi, M. A. Borden, *Bubble Sci. Eng. Technol.* **2009**, *1*, 3 – 17; F. Kiessling, S. Fokong, P. Koczera, W. Lederle, T. Lammers, *J. Nucl. Med.* **2012**, *53*, 345 – 348.
[8] G. Mees, R. Dierckx, C. Vangestel, C. Van de Wiele, *Eur. J. Nucl. Med. Mol. Imaging* **2009**, *36*, 1674 – 1686.
[9] I. R. Baird, K. A. Skov, B. R. James, S. J. Rettig, C. J. Koch, *Synth. Commun.* **1998**, *28*, 3701 – 3709.
[10] P. Kogan, R. Gessner, P. A. Dayton, *Bubble Sci. Technol.* **2010**, *2*, 3 – 8.
[11] J. Benjamins, A. Cagna, E. H. Lucassen Reynders, *Colloids Surf. A* **1996**, *114*, 245 – 254.
[12] P. N. Nguyen, T. T. Trinh Dang, G. Waton, T. Vandamme, M. P. Krafft, *ChemPhysChem* **2011**, *12*, 2646 – 2652.
[13] P. N. Nguyen, G. Waton, T. Vandamme, M. P. Krafft, *Angew. Chem. Int. Ed.* **2013**, *52*, 6404 – 6408; *Angew. Chem.* **2013**, *125*, 6532 – 6536.
[14] F. Gerber, M. P. Krafft, T. F. Vandamme, M. Goldmann, P. Fontaine, *Biophys. J.* **2006**, *90*, 3184 – 3192.
[15] S. Rossi, G. Waton, M. P. Krafft, *Langmuir* **2010**, *26*, 1649 – 1655; C. Szíjjártó, S. Rossi, G. Waton, M. P. Krafft, *Langmuir* **2012**, *28*, 1182 – 1189.
[16] J. J. Kwan, M. A. Borden, *Langmuir* **2010**, *26*, 6542 – 6548.

Received: March 26, 2015
Revised: April 21, 2015
Published online: June 9, 2015

 © 2015 Wiley-VCH Verlag GmbH & Co. KGaA, Weinheim